

Dynamics of a two-component atomic Bose-Einstein condensate

Ping Zhang¹, C.K. Chan², Xiang-Gui Li³, Xian-Geng Zhao¹

¹*Institute of Applied Physics and Computational Mathematics, Beijing
100088, China*

²*Department of Applied Mathematics, The Hong Kong Polytechnic University,
Kowloon, Hong Kong*

³*Department of Applied Mathematics, University of Petroleum, Shandong
257062, China*

The dynamical population oscillations between two internal states of a Bose-Einstein condensate are investigated within the rotating wave approximation. Analytical expressions for the population imbalance in the number states and coherent states have been derived, which predict different revival periods. Thus the true quantum state of the condensates may be unambiguously determined by detecting the atom intensity evolution for one internal state.

PACS: 03.75 Fi, 05.30 -d, 32.80.Pj, 74.20.D

Keywords: Bose-Einstein condensates, collapse and revival, Rabi oscillation.

The experimental observation of the Bose-Einstein condensation of a trapped, dilute gas of alkali atoms, and the high accuracy of the engineering, are opening a new avenue to investigate the interplay between macroscopics and quantum coherence. In particular, recent experiments on two-component Bose-Einstein condensates (BECs) in ⁸⁷Rb [1,2] have stimulated considerable theoretical work on the dynamics of the phase and number fluctuations of Bose condensates. Vigorous efforts have concentrated on the issue of temporal phase coherence between two coupled Bose condensates. Along semiclassical (mean) analysis much attention has focused on the coherent phenomena such as Josephson effect and macroscopic quantum self-trapping (MQST) [3,4,5,6]. Studies involving small quantum corrections show that due to the nonlinearities arising from the atom-atom interactions and the discrete spectrum of the many-body system, the dynamics of the population oscillations arising in the

mean-field approximation is modulated by the collapses and revivals [3,7,8,9,10,11,12,13].

In the present work, we study quantum dynamics of a two-component atomic BEC such as ^{87}Rb . Our purpose is to provide an analysis on how the coherent atom oscillations between two components depend on the initial states chosen for the condensates. We chose two different initial states of the condensate. In the first example we consider Fock state for each component of the condensate. In this case, we show that the revival period depends on whether the total atom number N is even or odd. In the other example we invoke Bose-broken symmetry and consider the product of two coherent states. In this case we show that the revival period is always definite. In experiments, such as ^{87}Rb , initial Fock states can be created by condensing independently two thermal atomic clouds trapped in different Zeeman level. Whereas, the initial coherent state may be created by splitting a condensate (trapped, say, in the Zeeman state $|f = 2, m_f = 2\rangle$) in two condensates trapped in the Zeeman states $|f = 2, m_f = 2\rangle$ and $|f = 2, m_f = 1\rangle$, respectively. Another aspect we are interested in this paper is the dependence of the coherent atom oscillations on the relative phase between two internal states and nonlinear atomic collisions.

We consider here Bose-Einstein condensation of a trapped gas of atoms that have two internal states $|1\rangle$ and $|2\rangle$ with energies $\hbar\omega_o/2$ and $-\hbar\omega_o/2$, respectively. There is a spatially uniform radiation field with frequency ω_e that couples the two internal states with a Rabi frequency Ω_0 . The atoms in states $|1\rangle$ and $|2\rangle$ are subject to isotropic harmonic trapping potentials $V_i(\mathbf{r}) = \frac{1}{2}m\omega_i r^2$ for $i = \{1, 2\}$, respectively. Furthermore, the atoms interact via elastic two-body collisions through the interaction potentials $V_{ij}(\mathbf{r} - \mathbf{r}') = \frac{4\pi\hbar^2 a_{ij}}{m}\delta(\mathbf{r} - \mathbf{r}')$, Where a_{ij} is the s -wave scattering length between atoms in states i and j . It is assumed that $a_{ij} > 0$ corresponding to repulsive interactions. In the formalism of second quantization, the system is described by the Hamiltonian

$$\widehat{H} = \widehat{H}_{atom} + \widehat{H}_{coll}, \quad (1a)$$

$$\widehat{H}_{coll} = \int d^3r \left\{ \frac{4\pi\hbar^2 a_{11}}{2m} \widehat{\Psi}_1^+(\mathbf{r}) \widehat{\Psi}_1^+(\mathbf{r}) \widehat{\Psi}_1(\mathbf{r}) \widehat{\Psi}_1(\mathbf{r}) \right.$$

$$\begin{aligned}
& + \frac{4\pi\hbar^2 a_{22}}{2m} \widehat{\Psi}_2^+(\mathbf{r}) \widehat{\Psi}_2^+(\mathbf{r}) \widehat{\Psi}_2(\mathbf{r}) \widehat{\Psi}_2(\mathbf{r}) \\
& + \frac{4\pi\hbar^2 a_{12}}{m} \widehat{\Psi}_1^+(\mathbf{r}) \widehat{\Psi}_2^+(\mathbf{r}) \widehat{\Psi}_1(\mathbf{r}) \widehat{\Psi}_2(\mathbf{r}) \}, \tag{1b}
\end{aligned}$$

$$\begin{aligned}
\widehat{H}_{atom} = & \int d^3r \{ \widehat{\Psi}_1^+(\mathbf{r}) \left[-\frac{\hbar^2}{2m} \nabla^2 + V_1(\mathbf{r}) + \frac{\hbar\delta}{2} \right] \widehat{\Psi}_1(\mathbf{r}) \\
& + \widehat{\Psi}_2^+(\mathbf{r}) \left[-\frac{\hbar^2}{2m} \nabla^2 + V_2(\mathbf{r}) - \frac{\hbar\delta}{2} \right] \widehat{\Psi}_2(\mathbf{r}) \\
& + \frac{\hbar\Omega_0}{2} (\widehat{\Psi}_1^+(\mathbf{r}) \widehat{\Psi}_2(\mathbf{r}) + \widehat{\Psi}_2^+(\mathbf{r}) \widehat{\Psi}_1(\mathbf{r})) \}. \tag{1c}
\end{aligned}$$

Here, the atomic field operators $\widehat{\Psi}_i(\mathbf{r})$ and $\widehat{\Psi}_i^+(\mathbf{r})$ have been written in the field interaction representation which is rotating at the frequency of the external field ω_e , $\delta = \omega_0 - \omega_e$ denotes the field detuning from resonance excitation.

Now we can approximate the field operators in the zero-temperature limit by a two-mode model such that $\widehat{\Psi}_i(\mathbf{r}) \approx \widehat{c}_i \phi_i(\mathbf{r})$, where \widehat{c}_i is the annihilation operator which obeys the usual boson commutation relations. In the two-mode approximation the Hamiltonian becomes (with $\hbar = 1$),

$$\begin{aligned}
\widehat{H} = & \left(\frac{1}{2}\delta + E_1\right) \widehat{c}_1^+ \widehat{c}_1 + \left(-\frac{1}{2}\delta + E_2\right) \widehat{c}_2^+ \widehat{c}_2 + \frac{\Omega}{2} (\widehat{c}_1^+ \widehat{c}_2 + \widehat{c}_2^+ \widehat{c}_1) \\
& + \frac{\kappa_{11}}{2} \widehat{c}_1^{+2} \widehat{c}_1^2 + \frac{\kappa_{22}}{2} \widehat{c}_2^{+2} \widehat{c}_2^2 + \kappa_{12} \widehat{c}_1^+ \widehat{c}_1 \widehat{c}_2^+ \widehat{c}_2, \tag{2}
\end{aligned}$$

where

$$E_i = \int d^3r \phi_i^*(\mathbf{r}) [-\nabla^2/(2m) + V_i(\mathbf{r})] \phi_i(\mathbf{r}), \tag{3a}$$

$$\Omega = \Omega_0 \int d^3r \phi_2^*(\mathbf{r}) \phi_1(\mathbf{r}), \tag{3b}$$

$$\kappa_{ij} = \frac{4\pi a_{ij}}{m} \int d^3r |\phi_i(\mathbf{r})|^2 |\phi_j(\mathbf{r})|^2. \tag{3c}$$

The analysis of Eq. (2) is greatly simplified by the introduction of the angular momentum operators

$$\widehat{J}_x = \frac{1}{2} (\widehat{c}_2^+ \widehat{c}_2 - \widehat{c}_1^+ \widehat{c}_1), \tag{4a}$$

$$\hat{J}_y = \frac{i}{2}(\hat{c}_2^+ \hat{c}_1 - \hat{c}_1^+ \hat{c}_2), \quad (4b)$$

$$\hat{J}_z = \frac{1}{2}(\hat{c}_1^+ \hat{c}_2 + \hat{c}_2^+ \hat{c}_1). \quad (4c)$$

The Casimir invariant is therefore

$$\hat{J}^2 = \frac{\hat{N}}{2}(\frac{\hat{N}}{2} + 1), \quad (5)$$

where $\hat{N} = \hat{c}_1^+ \hat{c}_1 + \hat{c}_2^+ \hat{c}_2$ is the total number operator, which is a constant of motion and thus can be set equal to the total number of atoms N . Therefore the present two-mode approximation is transformed into an angular momentum model with total angular momentum given by $j = N/2$. In terms of angular momentum operators the Hamiltonian (2) may be rewritten as

$$\hat{H} = \Omega \hat{J}_z + 2\kappa \hat{J}_x^2 + f(j), \quad (6)$$

where

$$\kappa = \frac{1}{2}(\frac{\kappa_{11}}{2} + \frac{\kappa_{22}}{2} - \kappa_{12}), \quad (7a)$$

$$\kappa' = \frac{1}{2}(\frac{\kappa_{11}}{2} + \frac{\kappa_{22}}{2} + \kappa_{12}), \quad (7b)$$

$$f(j) = 2\kappa' j^2 + (E_1 + E_2 - \kappa - \kappa')j. \quad (7c)$$

In deriving Eq. (6) we have assumed that

$$E_1 + \delta - E_2 + (\frac{\kappa_{11}}{2} - \frac{\kappa_{22}}{2})(2j - 1) = 0, \quad (8)$$

a condition that can always be achieved by adjusting field detuning δ and shifting the energy levels of the condensate components. Note that some control of the nonlinear parameter κ can be achieved through the proper engineering of the trapping potential or tuning the scattering lengths via Feshbach resonances.

In general the Hamiltonian (6) is difficult to treat in an exact way because of the presence of nonlinear atomic interactions. In order to gain physical insight into the dynamics of such a two-component BEC problem, some approximations are necessary: a common assumption [14,15] is the so-called rotating wave approximation (**RWA**) $\hat{U} = e^{-i\Omega t \hat{J}_z}$. Using the operator identity

$$\exp(i\lambda \hat{J}_z) \hat{J}_x \exp(-i\lambda \hat{J}_z) = \hat{J}_x \cos \lambda - \hat{J}_y \sin \lambda, \quad (9)$$

the Hamiltonian in the rotating frame (**RF**) becomes

$$\begin{aligned} \hat{H}_{RF} &= \hat{U}^\dagger \hat{H} \hat{U} + i \frac{d\hat{U}^\dagger}{dt} \hat{U} \\ &= \frac{1}{2} \kappa (e^{2i\Omega t} \hat{J}_+^2 + e^{-2i\Omega t} \hat{J}_-^2 + \hat{J}_+ \hat{J}_- + \hat{J}_- \hat{J}_+) + f(j), \end{aligned} \quad (10)$$

where $\hat{J}_\pm = \hat{J}_x \pm i\hat{J}_y$ are raising and lowering operators. Now we invoke **RWA** by suppressing rapidly oscillating time-dependent terms in Eq. (10). Thus we obtain the **RWA** Hamiltonian in the rotating frame as follows

$$\hat{H}_{RF}^{(r)} = -\kappa \hat{J}_z^2 + g(j), \quad (11)$$

where $g(j) = \kappa j^2 + f(j)$. Instead of discussing dynamics in the rotating frame, we return to the Hamiltonian in the previous field interaction representation

$$\hat{H}_{eff} = \hat{U} \hat{H}_{RF}^{(r)} \hat{U}^\dagger - i \frac{d\hat{U}^\dagger}{dt} \hat{U} = -\kappa \hat{J}_z^2 + \Omega \hat{J}_z + g(j), \quad (12)$$

which is our starting Hamiltonian for the following discussions. It reveals in Eq. (12) that \hat{J}_z is now a constant of motion and solely determined by the initial condition. The frozen \hat{J}_z behavior can be understood when Ω is sufficiently larger than κ , i.e., $\Omega \gg \kappa$. In this case, the external field forces the total spin to remain polarized in the z -direction because it costs energy to change the spin direction. To see the validity of our **RWA** Hamiltonian, we numerically integrate the Schrödinger equation with the original Hamiltonian (6) and present in Fig. 1(a) the expectation values $\langle \hat{J}_z \rangle$ against time for various values of Ω with the initial angular momentum state $|j, -j\rangle_x$ where the subscript denotes the quantization axis along

the x direction. We remark that for the system starts from $|j, -j\rangle_x$, the only nonvanishing spin component is \hat{J}_z because $\langle \hat{J}_x \rangle = \langle \hat{J}_y \rangle = 0$ at all times. Clearly it reveals in Fig. 1(a) that when $\Omega = 0$, $\langle \hat{J}_z \rangle$ vanishes after some time, which means that the initial coherence and polarization of \hat{J}_z is completely destroyed by the phase diffusion due to nonlinear term $2\kappa\hat{J}_x^2$. However, when Ω is sufficiently larger than κ , the value of $\langle \hat{J}_z \rangle$ remains almost unchanged during time evolution, consistent with Eq. (12) in which \hat{J}_z is a constant of motion. As a further illustration we calculate the energy spectrums of the two Hamiltonians and present the results in Fig. 1(b). It is found in calculations that the difference between the energies of two Hamiltonians approaches to be negligible when increasing the value of Ω . Thus we expect that the **RWA** Hamiltonian is valid in the parameter regime $\Omega \gg j\kappa$. In the following we will neglect the constant term $g(j)$ because this term denotes a simple constant energy shift and has no contribution to the dynamics of the system.

Now the Heisenberg equations of motion for the raising and lowering operators ($\hat{J}_\pm = \hat{J}_x \pm i\hat{J}_y$) can be readily solved as follows

$$\hat{J}_+(t) = e^{it(-2\kappa\hat{J}_z + \kappa + \Omega)} \hat{J}_+, \quad (13a)$$

$$\hat{J}_-(t) = e^{it(2\kappa\hat{J}_z + \kappa - \Omega)} \hat{J}_-. \quad (13b)$$

Given the initial state $|\psi(0)\rangle$ of the system, a quantity tailored to the dynamics is the population imbalance between the two components

$$\begin{aligned} N_-(t) &= 2\langle \psi(0) | \hat{J}_x(t) | \psi(0) \rangle \\ &= e^{i(\kappa + \Omega)t} \langle \psi(0) | e^{-2i\kappa t \hat{J}_z} \hat{J}_+ | \psi(0) \rangle + c.c.. \end{aligned} \quad (14)$$

Number state description. We shall now proceed to demonstrate how the population imbalance evolves for two different kinds of initial states of the condensates. First we consider the case that the condensate is in the Fock (number) states, equally the angular momentum states $|j, m\rangle_x$ where the value of $2m$ gives the atom number difference between the two BECs. We suppose that the condensates are initially localized in one well, corresponding to the state $|j, j\rangle_x$. Substituting this initial state into Eq. (14) gives

$$\begin{aligned}
N_-(t) &= e^{i(\kappa+\Omega)t} \sum_{m=-j}^j \sqrt{(j+m)(j-m+1)} \\
&\quad \times d_{j,m}^j\left(-\frac{\pi}{2}\right) d_{m-1,j}^j\left(\frac{\pi}{2}\right) e^{-i2\kappa mt} + c.c.,
\end{aligned} \tag{15}$$

where the matrix elements $d_{m,m'}^j(\theta) = \langle j, m | \exp(-i\theta \hat{J}_y) | j, m' \rangle$. Using the identity

$$d_{j,m}^j(\theta) = (-)^{j-m} \binom{2j}{j+m}^{1/2} \left(\cos \frac{\theta}{2}\right)^{j+m} \left(\sin \frac{\theta}{2}\right)^{j-m}, \tag{16}$$

and recursive relation

$$d_{j,m}^j(\theta) = -\frac{\sin(\theta/2)}{\cos(\theta/2)} \left(\frac{j+m+1}{j-m}\right)^{1/2} d_{j,m+1}^j(\theta), \tag{17}$$

we obtain

$$\begin{aligned}
N_-(t) &= \frac{1}{2^N} e^{i(\kappa+\Omega)t} e^{i2j\kappa t} \sum_{m=-j}^j (j+m) \binom{2j}{j+m} e^{-i2\kappa(j+m)t} + c.c. \\
&= N[\cos(\kappa t)]^{N-1} \cos(\Omega t).
\end{aligned} \tag{18}$$

From Eq. (18) one can see that the population imbalance involves a rapidly oscillating part and an envelope function that is responsible for the collapse and revival of the population imbalance. The most prominent feature in Eq. (18) is that the parity of total atom number N , whether it is odd or even, plays an essential role in determining revival periods. When N is odd, the revival period is π/κ , and the population imbalance is always larger than zero. That is, the population undergoes the macroscopic quantum self-trapping. However, when the number of atoms is even, $N-1$ is odd and the condensate will undergo antirevivals when $t = (2n+1)\pi/\kappa$ so that $N_-(t) = -N$ at these times. In this case, the revival period becomes $2\pi/\kappa$ and the time average of $N_-(t)$ is zero. Two examples are plotted in Figs. 2(a)-(b). To show the validity of the analytical results of Eq. (18) which is derived from the **RWA** Hamiltonian, we numerically calculate the Schrödinger equation with the original Hamiltonian (6). The results are shown in Fig. 2(c)-(d), corresponding to Fig. 2(a)-(c), respectively. Clearly, the **RWA** formula, equation (18), describes the system's evolution very well when compared with the exact numerical results shown in Fig. 2(c)-(d), implying

the different periods of quantum revivals for different parities of N . We notice that the reduction in revival amplitude shown in Fig. 2(c)-(d) is due to the state mixing induced by angular momentum operator \hat{J}_x , which is eliminated in the RWA treatment. If the Fock states with a fixed number of atoms are appropriate for the description of the condensates, then by monitoring the initially unoccupied internal state using off-resonant light scattering, this change for the magnitude of the revival period of the population imbalance between the two components may be observed. A similar phenomenon has been discussed in Ref.[16] in the context of the interference pattern, without considering coupling and nonlinear atomic collision between the two components. However, because the visibility of the interference pattern is never negative, so the revival period considered in Ref.[16] is always π/κ with a π phase shift for different parities of N .

Coherent state description. We turn now to the coherent state description of the problem. It is customary to consider the condensates to be in two coherent states, associated with a macroscopic wave function with both magnitude and phase, the presence of which is due to the spontaneous breaking of gauge symmetry. This is the view we will adopt here, to assume the condensate to be such coherent states with definite relative phase

$$|\psi(0)\rangle = |\alpha, \beta\rangle. \quad (19)$$

The amplitude of the two components may be presented by $|\alpha| = \sqrt{N} \sin(\theta)$ and $|\beta| = \sqrt{N} \cos(\theta)$, conserving total atom number. The relative phase between the two components is defined to be ϕ . Thus the two complex amplitudes are related by $\beta\alpha^* = \frac{1}{2}N \sin(2\theta) \exp(i\phi)$. To give a closed expression for Eq. (14) with the initial state Eq. (19), we need the normal-ordering arrangement for the operator function $\exp(\lambda\hat{J}_z)\hat{J}_+$. With the aid of the following identity

$$e^{-\lambda\hat{c}_i^+\hat{c}_i} = \sum_{r=0}^{\infty} \frac{x^r}{r!} \hat{c}_i^{+r} \hat{c}_i^r, \quad (20)$$

where $x = e^{-\lambda} - 1$, and after a straightforward calculation, we obtain

$$e^{2\lambda\hat{J}_z}\hat{J}_+ = \frac{1}{2}e^{\lambda(\hat{c}_2^+ + \hat{c}_1^+)} \sum_{m,n,p,q=-\infty}^{\infty} \left\{ \frac{x^m x^n y^q z^p}{m!n!p!q!} \right.$$

$$\begin{aligned}
& \times \hat{c}_1^{+m} \hat{c}_1^{+n} \hat{c}_2^{+p} \hat{c}_2^{+q} \left[\sum_{l=-\infty}^{\infty} \frac{z^l}{l!} (\hat{c}_2^+ + \hat{c}_1^+)^l (\hat{c}_2 - \hat{c}_1)^l \right] \\
& \times \hat{c}_1^m \hat{c}_1^p \hat{c}_2^n \hat{c}_2^q \} (\hat{c}_2 - \hat{c}_1),
\end{aligned} \tag{21}$$

where $y = (e^{2\lambda} + 1)/2$, and $z = (e^{2\lambda} - 1)/2$. Substituting Eqs. (20)-(21) into Eq. (14), we have the final result for the population imbalance at time t in the coherent state representation

$$N_-(t) = A \exp\left(-2N \sin^2 \frac{\kappa t}{2}\right) \cos[W \sin(\kappa t) + \Omega t + \varphi], \tag{22}$$

where we have defined $A = N \sqrt{1 - \cos^2 \phi \sin^2(2\theta)}$, $W = -N \sin(2\theta) \cos \phi$, and a constant phase shift $\varphi = \arctan[\sin \phi \tan(2\theta)]$. We can see from Eq. (22) that the dynamics of the population imbalance is mainly determined by the envelope function $\exp(-2N \sin^2 \frac{\kappa t}{2})$, with modulated by a rapidly varying cosine term. The characteristics of collapses and revivals can be clearly seen from Eq. (22). For comparison with Eq. (18) derived in the number state space, let us chose the value of $\theta = 0$, corresponding the case that the condensate is initially localized in one internal state. Then $N_-(t)$ in Eq. (22) reduces to

$$N_-(t) = N \exp\left(-2N \sin^2 \frac{\kappa t}{2}\right) \cos(\Omega t). \tag{23}$$

Although no relative phase information occurs in Eq. (23), quite different from number states, revivals for the condensate in the coherent states occur at definite times $t = 2\pi n/\kappa$ (n is an integer), independent of the parities of the average particle number N . As illustrated in Ref.[16], this difference of revival periods between the Fock state and coherent state descriptions originates from the fact that the atom number difference operator $\hat{c}_2^+ \hat{c}_2 - \hat{c}_1^+ \hat{c}_1$ is quantized in units of 2 when the condensates are in Fock states and units of 1 for coherent states.

We emphasize here that for any realistic experimental set up, the exact atom number is unknown and maybe has a large number fluctuation over many different experimental runs. As a result, what we obtain in Fock states should be wieghted by a factor $p(N)$ describing the probability the state $|j, j\rangle_x$ occurs at the begaining. According to quantum measurement theory, however, the atom number in any given experiment would be well defined. Thus

in the Fock-state description, the occurrence of antirival phenomenon, which features the parity of the atom number, is robust for any single experiment. On the other hand, the antirevival phenomenon never occurs in the coherent-state description, which can be seen from Eq. (23). This is because the coherent state is a superposition of the Fock states with the weighting factor satisfying the Poisson number distribution. Consequently, in each single experiment quantum fluctuations will be present in the coherent state description, which smears out the antirevivals. This fact allows us the possibility to detect the true quantum state of the two-component BEC system in realistic experiment.

In the case of the values of nonlinear interactions satisfying the following condition

$$\kappa = \frac{1}{2} \left(\frac{\kappa_{11}}{2} + \frac{\kappa_{22}}{2} - \kappa_{12} \right) \equiv 0, \quad (24)$$

our RWA treatment of Hamiltonian (6) is exact and Eq. (22) reduces to description of a simple Rabi oscillation with period $2\pi/\Omega$. This form of atomic collective excitation has been observed in Ref.[2]. The existence of Rabi oscillation also depends on the initial state conditions, which is reflected by the fact that the oscillation amplitude A in Eq. (22) is determined by the initial population distribution and relative phase between the two components. In particular when the value of $\theta = \pi/4$, corresponding to equal atom distribution between the two internal states, and $\phi = n\pi$, we arrive at the conclusion that the oscillation is completely suppressed and no quantum tunneling occurs during time evolution. Note that the present conditions of zero oscillation is identical to the fixed points discussed in Ref.[5], in which the semiclassical approximation has been adopted. In general the value of effective interaction κ is not zero and it can be adjusted through the proper engineering of the trapping potential, and hence of the condensate wave functions $\phi_i(\mathbf{r})$. To illustrate the interplay between the weak nonlinearity and strong Josephson-like coupling, we present in Fig. (3) $N_-(t)$ [Eq. (23)] for several values of κ . It reveals in Fig. (3) that the presence of the effective nonlinear interaction modulates the fringe visibility of the internal Rabi oscillations as a manner of collapses and revivals, as has been verified by JILA group [2]. When κ increases to large values, the rapid phase diffusion caused by the nonlinear interaction

destroys the collective excitation of atoms, corresponding to the complete smearing of the Rabi oscillations, as illustrated in Fig. 3(d).

To see the effect of the initial relative phase on the dynamics of the system, we present in Fig. 4 the time evolution of $N_-(t)$ for four different values of ϕ . The value of θ in these figures is chosen to be $\pi/4$, corresponding to the two condensates with equal atoms. We can see in Fig. 4 that the oscillation amplitude is maximal for the values $\phi = \pi/2$. Experimental observation of this change of oscillation amplitudes may help us determine the relative phase between the two condensates.

We have restricted our analysis to zero temperature. Our study of the effect of initial state selection on the consequent dynamics of a two-component condensate should be extended to finite temperatures, where dissipative effects associated with the thermal cloud of noncondensate atoms must be included. Further study of damping in this system is needed.

In summary, with the help of rotating wave approximation, we have derived analytical expressions for the population imbalance between the two Bose condensates in the number states and coherent states. The time evolution of the coherent atom oscillations is shown to be quite different between these two state descriptions. For the condensates in number states, the revival periods of the oscillations are either π/κ or $2\pi/\kappa$, depending on whether the total atom number is odd or even. Whereas, for the condensates in coherent states, the revival periods are always $2\pi/\kappa$. So the true quantum state of the condensates may be unambiguously determined by detecting the atom intensity evolution for one trap.

-
- [1] M.R. Andrews, C.G. Townsend, H.-J. Miesner, D.S. Durfee, D.M. Kurn, and W. Ketterle, *Science* **275**, 637 (1997).
- [2] D.S. Hall, M. R. Matthews, J. R. Ensher, C. E. Wieman, and E. A. Cornell, *Phys. Rev. Lett.* **81**, 1539 (1998).

- [3] G. J. Milburn, J. Corney, E. M. Wright, and D. F. Walls, Phys. Rev. A **55**, 4318 (1997).
- [4] A. Smerzi, S. Fantoni, S. Giovannazzi, and S.R. Shenoy, Phys. Rev. Lett. **79**, 4950 (1997).
- [5] S. Raghavan, A. Smerzi, S. Fantoni, and S.R. Shenoy, Phys. Rev. A **59**, 620 (1999).
- [6] J. Williams, R. Walser, J. Cooper, E. Cornell, and M. Holland, Phys. Rev. A **59**, R31 (1999).
- [7] P. Villain, M. Lewenstein, R. Dum, Y. Castin, L. You, A. Imamoglu, and T.A.B. Kennedy, J. Mod. Opt. **44**, 1775 (1997).
- [8] S. Raghavan, A. Smerzi, and V.M. Kenkre, Phys. Rev. A **60**, R1787 (1999).
- [9] J. Javanainen and M.Y. Ivanov, Phys. Rev. A **60**, 2351 (1999).
- [10] A. Smerzi and S. Raghavan, Phys. Rev. A **61**, 063601 (2000).
- [11] M. J. Steel and M.J. Collet, Phys. Rev. A **57**, 2920 (1998).
- [12] L.-M. Kuang and Z.-W. Ouyang, Phys. Rev. A **61**, 023604 (2000).
- [13] D. Gordon and C.M. Savage, Phys. Rev. A **59**, 4623 (1999).
- [14] A.P. Alodjanc, S.M. Arakeljan, and A.S. Chirkin, Zh. Eksp. Teor. Fiz. **108**, 63 (1995) [JETP **81**, 34 (1995)].
- [15] L.-M. Kuang, Z.-Y. Tong, Z.-W. Ouyang, and H.-S. Zeng, Phys. Rev. A **61**, 013608 (1999).
- [16] T. Wong, M.J. Collet, S.M. Tan, D.F. Walls, and E.M. Wright, cond-mat/9611101 (1996).

Figure captions

Fig. 1. (a) Time evolution of $\langle \hat{J}_z \rangle$ for the value of total atom number $N = 100$. The initial state is $|j, -j\rangle_x$; (b) energy spectrums of the exact Hamiltonian (closed triangles) and the **RWA** Hamiltonian (closed squares) for the values of $N = 100, \Omega = 30\kappa$.

Fig. 2. Analytical results of population imbalance $N_-(t)$ for the value of total atom number (a) $N = 100$ and (b) $N = 101$. The exact numerical results corresponding to (a) and (b) are shown in (c) and (d), respectively. Other parameters are $\kappa = 0.001\Omega$.

Fig. 3. Population imbalance $N_-(t)$ for the value of effective nonlinear coupling (a) $\kappa = 0$, (b) $\kappa = 0.001\Omega$, (c) $\kappa = 0.005\Omega$, and (d) $\kappa = 0.025\Omega$. Other parameters are $N = 100$ and $\theta = 0$.

Fig. 4. Population imbalance $N_-(t)$ for the value of relative phase (a) $\phi = 0$, (b) $\phi = \pi/6$, (c) $\phi = \pi/4$, and (d) $\phi = \pi/2$. Other parameters are $N = 100$ and $\kappa = 0.01\Omega$.

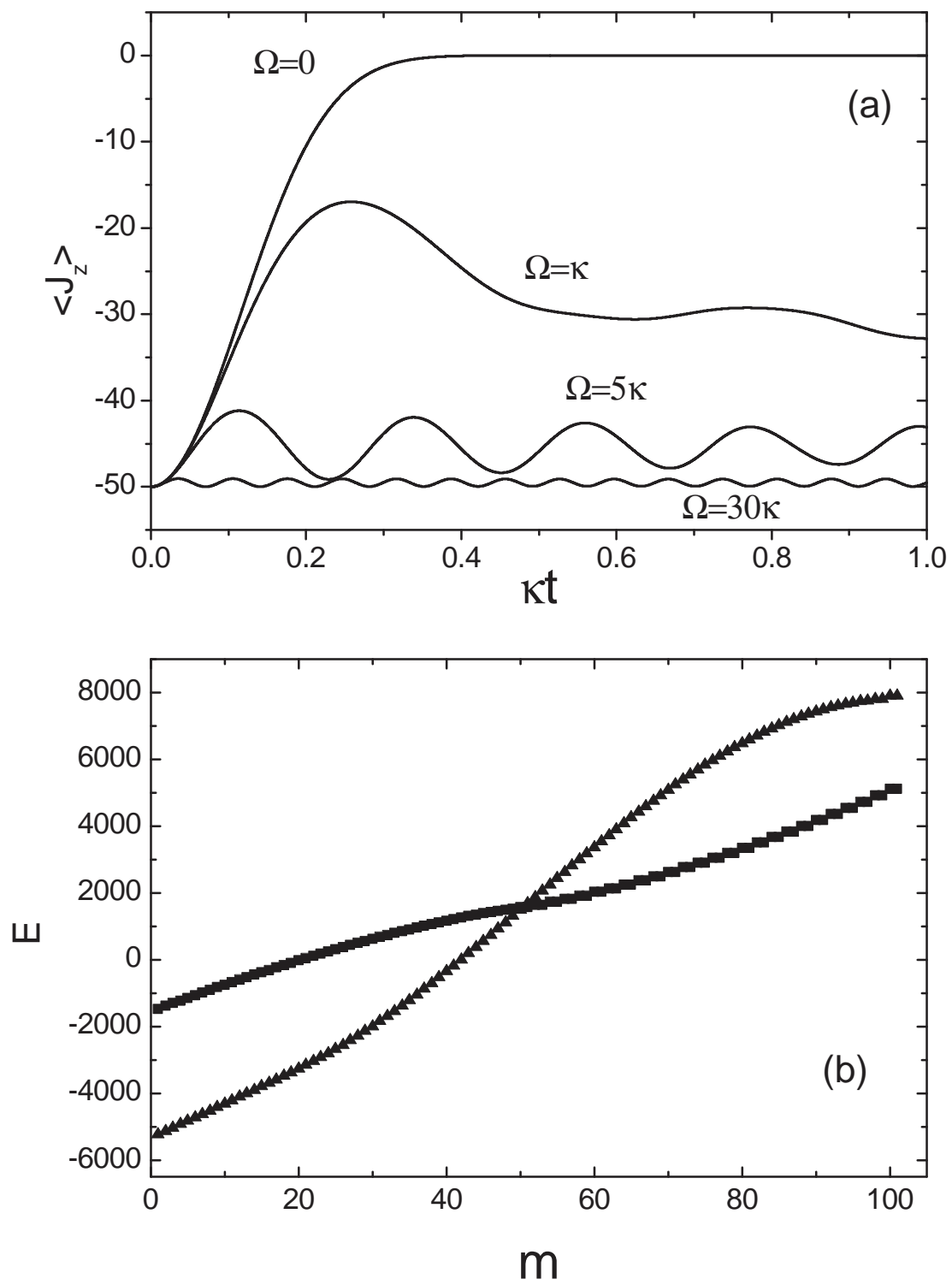


Fig. 1

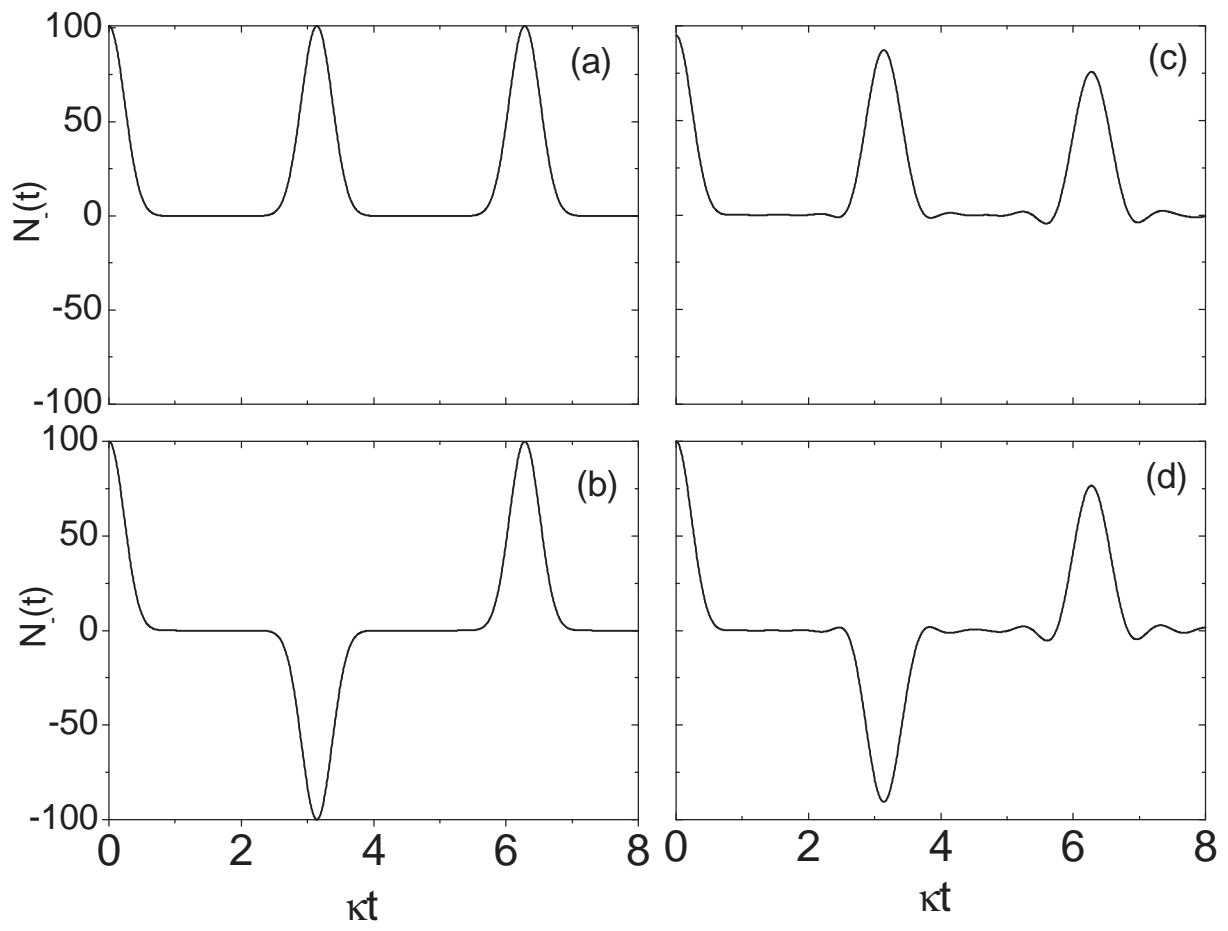


Fig. 2

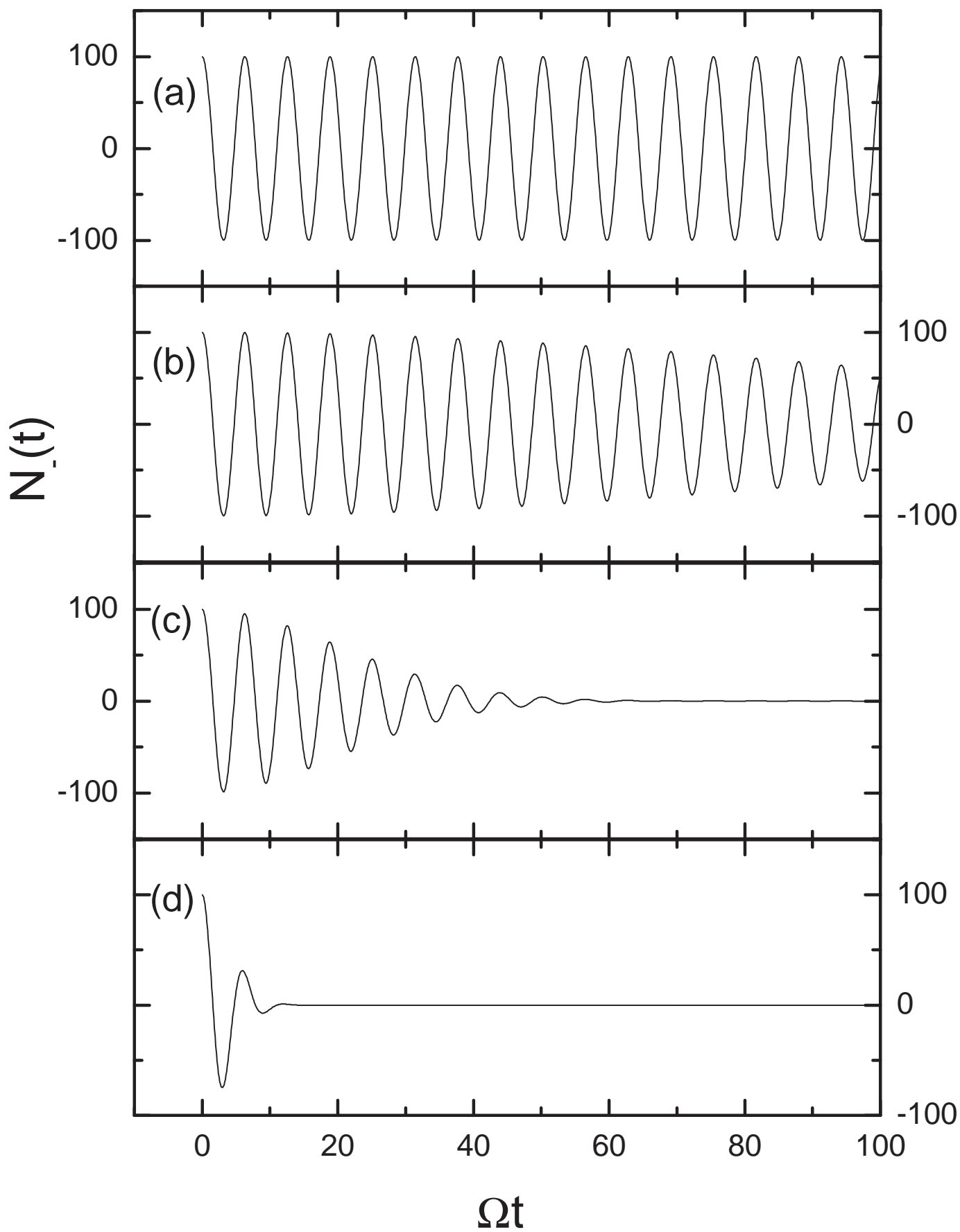


Fig. 3

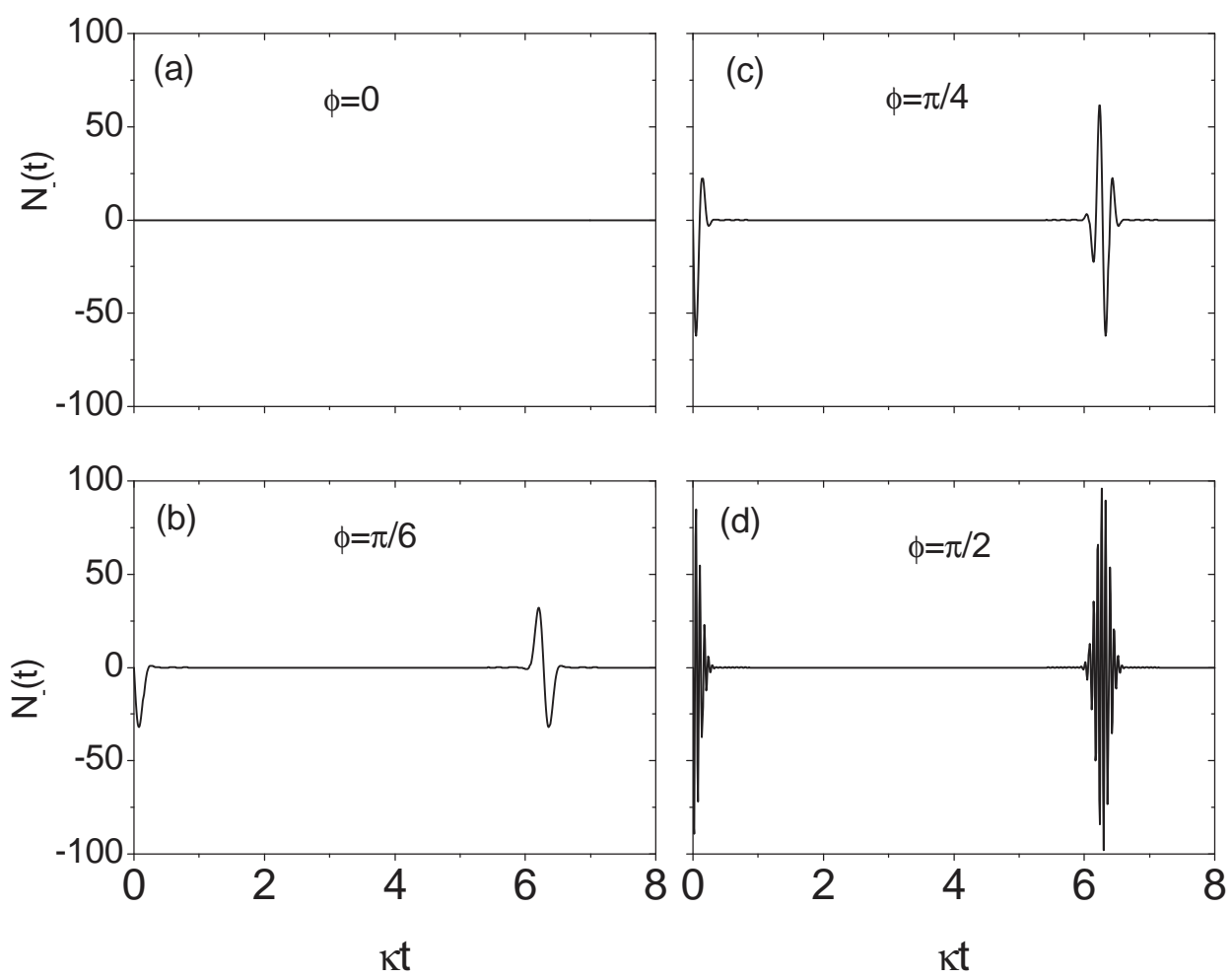


Fig. 4